Office of Naval Research

Contract Nonr-1866 (16) NR-372-012

NATIONAL AERONAUTICS AND SPACE ADMINISTRATION

Grant NGR 22-007-068

THE SEPARATE COMPUTATION OF ARCS FOR OPTIMAL FLIGHT PATHS WITH STATE VARIABLE INEQUALITY CONSTRAINTS

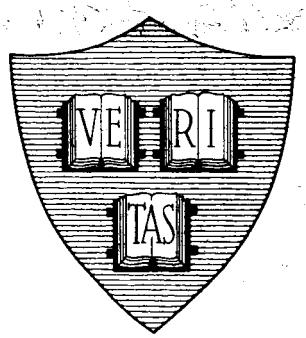

By

Jason L. Speyer, Raman K. Mehra and Arthur E. Bryson, Jr.

May 1967

Technical Report No. 526

Division of Engineering and Applied Physics

Harvard University • Cambridge, Massachusetts

Office of Naval Research

Contract Nonr-1866(16)

NR - 372 - 012

National Aeronautics and Space Administration

Grant NGR-22-007-068

THE SEPARATE COMPUTATION OF ARCS FOR OPTIMAL FLIGHT PATHS WITH STATE VARIABLE INEQUALITY CONSTRAINTS

By

Jason L. Speyer, Raman K. Mehra, and Arthur E. Bryson, Jr.

Technical Report No. 526

May 1967

The research reported in this document was made possible through support extended the Division of Engineering and Applied Physics, Harvard University by the U. S. Army Research Office, the U. S. Air Force Office of Scientific Research and the U. S. Office of Naval Research under the Joint Services Electronics Program by Contracts Nonr-1866(16), (07), and (32), and NASA Grant NGR-22-007-068.

Division of Engineering and Applied Physics

Harvard University Cambridge, Massachusetts

* THE SEPARATE COMPUTATION OF ARCS FOR OPTIMAL FLIGHT PATHS WITH STATE VARIABLE INEQUALITY CONSTRAINTS

By

Jason L. Speyer, Raman K. Mehra, and Arthur E. Bryson, Jr.

Division of Engineering and Applied Physics

Harvard University Cambridge, Massachusetts

ABSTRACT

Separate computation of arcs is possible for a large class of optimization problems with state variable inequality constraints. Surprisingly, this class (to the best of the authors' knowlege) includes all physical problems which have been solved analytically or numerically to date. Typically these problems have only one constrained arc. Even in more complex problems, separation of arcs can be used to search for additional constrained arcs.

As an important example, a maximum range trajectory for a glider entering the Earth's atmosphere at a supercircular velocity is determined, subject to a maximum altitude constraint after initial pull-up. It is shown that the optimal path can be divided into three arcs, which may be determined separately with no approximations. The three arcs are (1) the initial arc, beginning at specified initial condition and ending at the entry point onto the altitude constraint; (2) the arc lying on the altitude constraint; and (3)the terminal arc, beginning at the exit point of the altitude constraint and ending at some specified terminal altitude.

---

* The work reported was partially supported by the Space and Information Systems Division of the Raytheon Company.

ABSTRACT (Cont'd)

The conjugate gradient method, (ref. 4), a first order optimization scheme, is shown to converge very rapidly to the individual unconstrained optimal arcs. Using this optimization scheme and taking advantage of the separation of arcs an investigation revealed that two locally optimum paths exist. The range of one exceeds the range of the other by about 250 nautical miles (about 6%) for the re-entry vehicle used here (maximum lift-to-drag ratio is .9) .

I. INTRODUCTION

In the past few years techniques for solving optimal programming problems with a state variable inequality constraint (SVIC) have been developed. Necessary conditions for a stationary solution were given by Gamkrelidze [1], and Bryson, Denham, and Dreyfus, [2]. One numerical technique for solving such problems uses a "penalty function" which requires the introduction of an auxiliary state variable [3], [4]. An improvement over the "penalty function" method, in both speed and accuracy, is the direct approach [5], where the SVIC is satisfied without using an extra state variable. In both techniques, the equations of motion and the Euler-Lagrange equations must be integrated over the entire path for each iteration.

The present paper shows that for certain problems with a SVIC, the computation of the state and Euler-Lagrange variables need only be done on the unconstrained arcs. Numerical computation of shorter unconstrained paths allows more rapid convergence and increased numerical accuracy. Also, if the constrained arc forms a large part of the entire path, this

greatly reduces the amount of computation required. This separation of arcs occurs, for example, in the problem of finding the maximum range of a glider entering the Earth's atmosphere at parabolic velocities subject to a maximum altitude constraint after initial pull-up (sketch of possible trajectory in altitude-range space is shown in Fig. 1) . This problem was solved by the direct method of reference 5 and by the penalty function method in reference 11. The independence of the unconstrained arcs can be seen by observing that on the constant altitude constraint two of the three state variables are fixed (altitude and flight path angle); the velocity decreases due to the drag force. Velocity vs. range is a universal curve on this arc; only the velocity at the beginning and the end of this arc need be determined. A maximum range path, starting at any velocity on the constraint boundary that is higher than the velocity at the end of the constrained arc, has the same unconstrained path from the exit point of the altitude constraint to the terminal altitude. Similarly, a maximum range path, ending at any velocity on the constraint boundary that is lower than the velocity at the beginning of the constrained arc, has the same unconstrained path from the inital point to the entry point onto the constraint boundary. The unconstrained arcs can be found separately, determining the velocities at the beginning and the end of the constrained arc in the process. Having these velocities, the range on the altitude constraint can be easily evaluated. The three arcs put together form the maximizing path, without any approximations.

Such separation of arcs is possible if the number of variables on which the motion and constraints depend explicitly is larger by one than the order of the SVIC. The order of a SVIC is defined as the number of

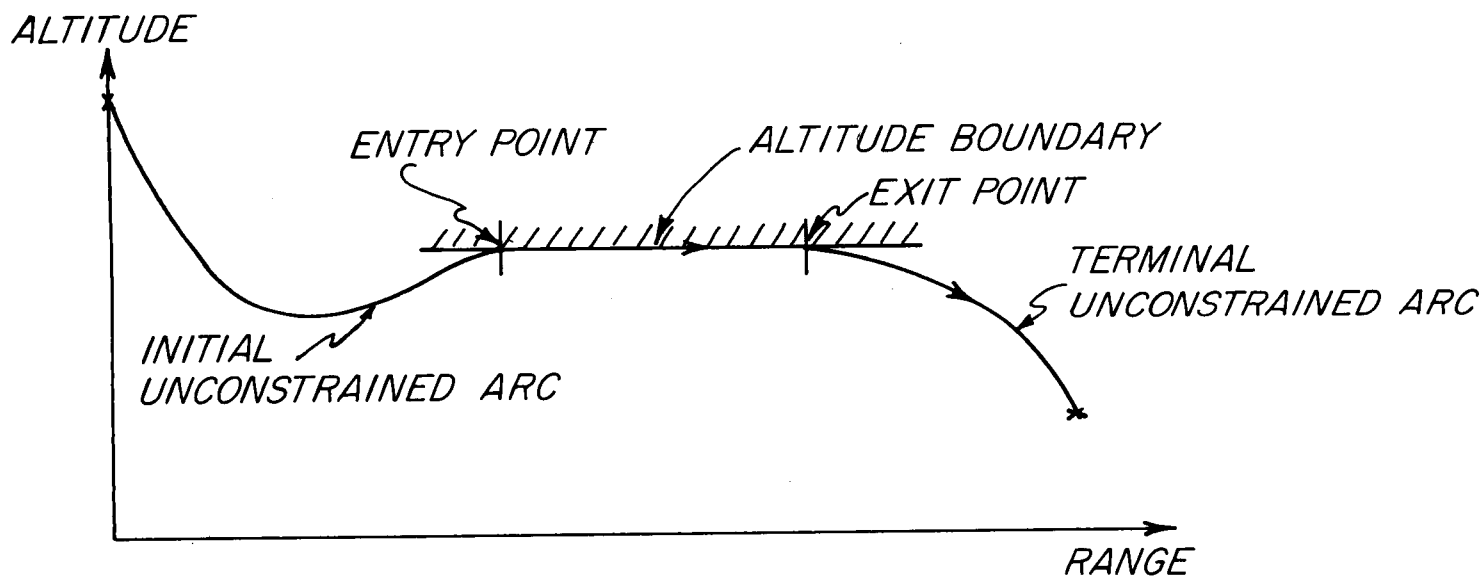

FIG. 1 SKETCH OF THE GLIDER'S TRAJECTORY IN ALTITUDE-RANGE SPACE.

differentiations of the SVIC function needed for the control variable to appear explicitly (cf. ref. 2)

2. PROBLEM FORMULATION

The general problem considered here is to determine a control program $u(t)$, in the interval $t_o \leqq t \leqq t_f$ so as to maximize

$$J = \int_{t_o}^{t_f} g(x, u, t)\, dt \tag{1}$$

subject to the constraints

$$\dot{x} = f(x, u, t) \tag{2}$$

$$M = M[x(t_f), t_f] \tag{3}$$

$$S(x, t) \leqslant 0 \tag{4}$$

$$t_o \text{ and } x(t_o) \text{ given} \tag{5}$$

where t (time) is the independent variable; $(\cdot)$ is $d/dt(\,)$; $u(t)$ is a scalar control variable; $x(t)$ is an n-vector of state variables; f is an n-vector of known functions of $x(t)$, $u(t)$, and t, and is assumed everywhere differentiable with respect to x and u; M is a q-vector of known functions of $x(t_f)$ and t_f, $q \leqslant n$; S is a scalar function of $x(t)$ and t.

For those intervals of time that an extremal solution lies on a p^{th} order SVIC boundary ($S(x, t) = 0$) it is necessary that S and all its time derivatives that do not contain the control be zero:

$$[S, \dot{S}, \ldots\ldots, S^{(p-1)}]^T = 0 \tag{6}$$

The value of the control which keeps (6) satisfied along the constrained path is obtained by the p^{th} derivative of S

$$S^{(p)}(x, u, t) = 0 \tag{7}$$

It is assumed that the control on the constraint boundary can be found as a function of (x, t) from the implicit equation (7) in the form

$$u = \Lambda (x, t) \tag{8}$$

3. SUFFICIENT CONDITIONS FOR SEPARATE COMPUTATION OF ARCS

Separation of arcs is possible if the contribution of the constrained arc to the performance index depends only on the entry and exit values of one variable (t or some element of x). Suppose the contribution of the constrained arc to the performance index, $J(t_1, t_2)$ is

$$J[t_1, t_2] = \int_{t_1}^{t_2} g(x, u, t)\, dt \tag{9}$$

where t_1 is the entry point time and t_2 is the exit point time. If p=n then (6) can be used to solve for all the variables in terms of one, say x_1. Let the remaining n-1 state variables be denoted by the vector y. Then from (6)

$$\begin{bmatrix} y \\ t \end{bmatrix} = r(x_1) \tag{10}$$

All the variables in (9) can be eliminated except x_1 if (y, t, u) are eliminated using (10) and (8) and the variable of integration is changed from t to x_1 by the differential element of x_1 in (2) as

$$\dot{x}_1 = f_1(x_1, y, t, u) \tag{11}$$

Thus (9) becomes

$$J[t_1, t_2] = \int_{x_1(t_1)}^{x_1(t_2)} \frac{g\{x_1,\ r[x_1], \Lambda\,[x_1, r(x_1)]\}}{f_1\{x_1,\ r(x_1), \Lambda\,[x_1, r(x_1)]\}}\ dx_1$$

$$= \int_{x_1(t_1)}^{x_1(t_2)} G(x_1)\ dx_1 = K[x_1(t_2)] - K[x_1(t_1)] \tag{12}$$

It is tacitly assumed that starting from any value of $x_1(t_1)$ on the constrained arc, the value of $x_1(t_2)$ will eventually be reached.

If (12) is possible then the optimization problem can be separated into two smaller optimization problems. They are; find u(t) to maximize

$$J_1 = J\ [t_o\ ,\ t_1] - K\ [x_1(t_1)] \tag{13}$$

subject to (2), (5) and the corner conditions of (6) and ; find u(t) to maximize

$$J_2 = J[t_2\ ,\ t_f] + K[x_1(t_2)] \tag{14}$$

subject to (2), (3) and the initial conditions of (6). The sum of (13) and (14) will give the maximum value of (1).

If the equations of motion and boundary conditions do not explicity depend upon clock time but only on time elapsed from the initial time, then the arcs will separate for $n-1 = p$.

4. MAXIMUM RANGE OF A HYPERSONIC GLIDER WITH AN ALTITUDE CONSTRAINT

The ideas of the previous section are applied here to the problem of

maximizing the range of a glider (entering the Earth's atmosphere* at parabolic speeds) with an inflight constraint on the maximum altitude after pull-up. This problem, originally thought to be a complicated problem with a SVIC (ref. 5), falls into the special class of separable problems.

The nomenclature for this problem is given in Fig. 2. The aerodynamic forces, lift and drag, are varied through the control variable $\alpha(t)$ = angle-of-attack. The lift-drag characteristics of the glider are shown in Fig. 3. The wing loading of the glider mg/S, was taken as 61.3 lb. ft^{-2}. The 1956 ARDC standard atmosphere model was used. The glider is approximated as a point mass moving about a spherical nonrotating Earth. The equations of motion are:

$$\dot{V} = \frac{-C_D \rho V^2 S}{2m} - g \sin \gamma \tag{15}$$

$$\dot{\gamma} = \frac{C_L \rho V S}{2m} + \left(\frac{V}{R + h} - \frac{g}{V} \right) \cos \gamma \tag{16}$$

$$\dot{h} = V \sin \gamma \tag{17}$$

The problem is to find the control program, $\alpha(t)$, which maximizes the range

$$R_A = \int_{t_o}^{t_f} \frac{V}{1 + h/R} \cos \gamma \, dt \tag{18}$$

subject to (15), (16), and (17), with initial conditions on V, γ, and h, and a

*Actually the problem is started in the Earth's atmosphere partly to save computer time and partly because the control force is negligible compared to the centrifugal force during most of the omitted path.

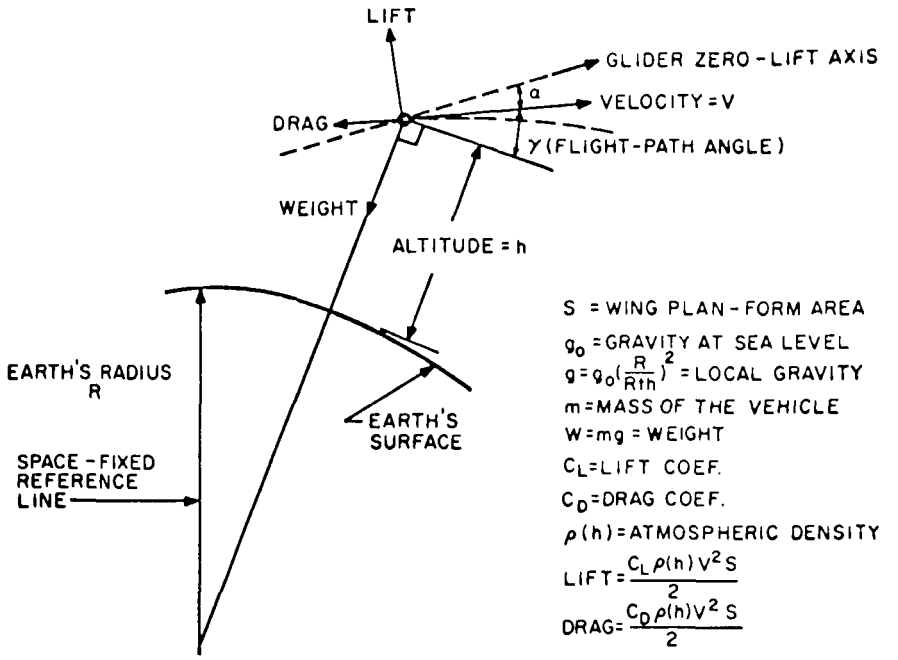

FIG. 2 GEOMETRY AND NOMENCLATURE OF ATMOSPHERIC RE-ENTRY EXAMPLE PROBLEM.

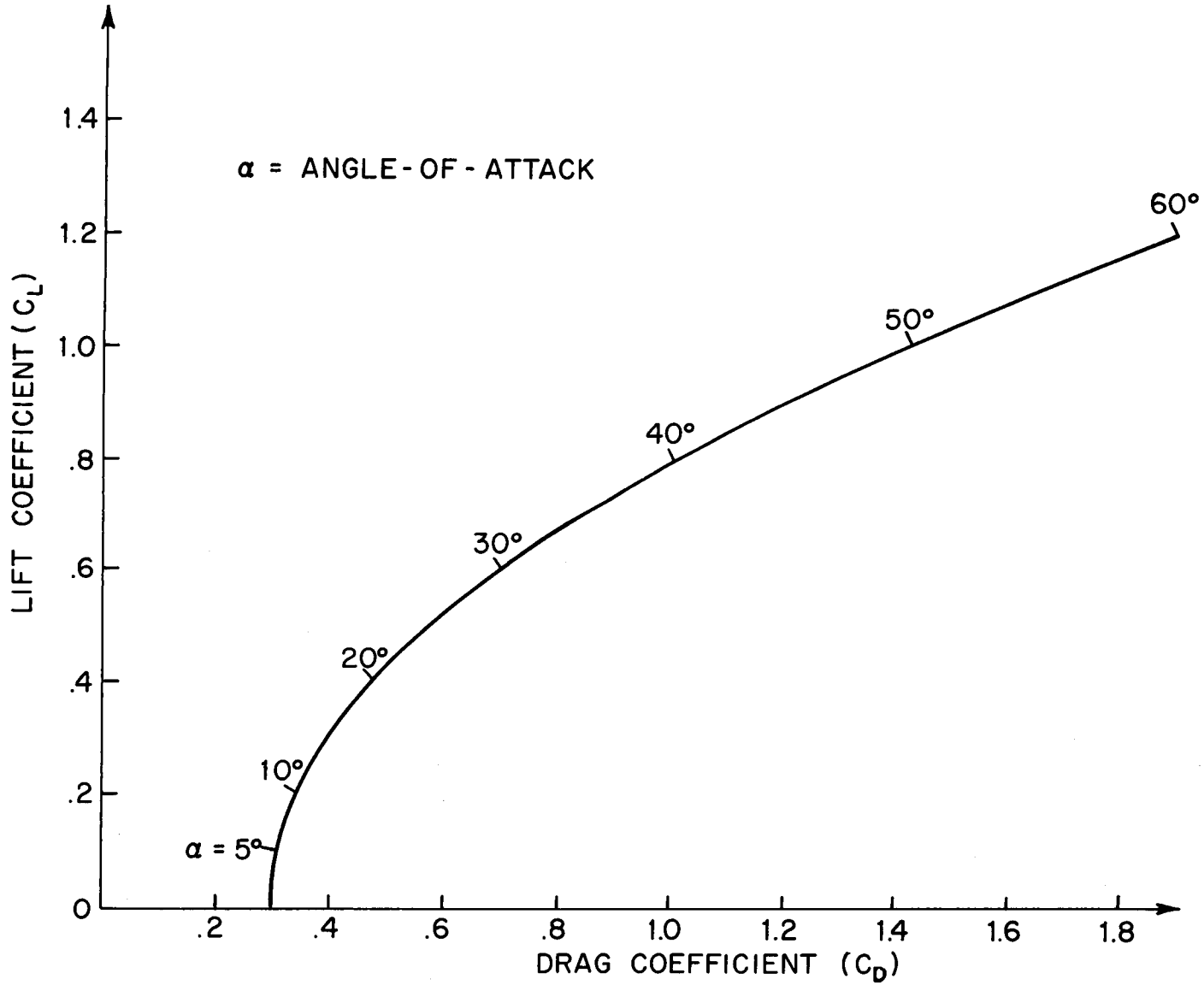

FIG. 3 LIFT-DRAG POLAR FOR RE-ENTRY VEHICLE

terminal condition on altitude and the inflight inequality constraint

$$h(t) \leq h_M \tag{19}$$

where h_M is the given value of the maximum allowable altitude.

5. SEPARATION OF ARCS FOR THE MAXIMUM RANGE PROBLEM

Starting from the initial conditions, a maximum range path eventually enters onto the constraint boundary at time t_1. At this point

$$h - h_M = 0 \tag{20}$$

$$\dot{h} = V \sin \gamma = 0 \tag{21}$$

must be satisfied as well as all along the constraint boundary. The control used to keep (20) and (21) satisfied on the constraint boundary is found from $\ddot{h} = 0$ which implies

$$C_L = \frac{2m}{\rho_M V S} \left[\frac{g_M}{V} - \frac{V}{R + h_M} \right] \tag{22}$$

where ρ_M and g_M are the values of ρ and g on the constraint boundary.

Since h and γ are fixed on the constraint boundary, only the velocity is free. The horizontal range travelled on the constraint boundary can be found as a function of the arc-entry and arc-exit velocities. The independent variable t is eliminated by (15) so that

$$R_A [t_1, t_2] = \int_{V(t_2)}^{V(t_1)} \frac{2m dV}{(1 + h_M/R) C_D \rho_M V S} = F[V(t_1)] - F[V(t_2)] \tag{23}$$

where C_D is a function only of velocity through (22) and Fig. 2. Conceptually $R_A(t_1, t_2)$ depends only on the values of the exit and entry velocities although in general an analytic expression cannot be found.

Thus the problem can be reduced to two smaller problems in which the unconstrained arcs are found separately. The initial unconstrained arc from the initial conditions to the entry point onto the constraint boundary is found by obtaining a $\alpha(t)$ which maximizes,

$$R_I = \int_{t_o}^{t_1} \frac{V \cos \gamma}{1+h/R} \, dt + F[V(t_1)] \tag{24}$$

The terminal unconstrained arc from the exit point of the constrained arc to the terminal boundary is found by evaluating an $\alpha(t)$ which maximizes

$$R_F = \int_{t_2}^{t_f} \frac{V \cos \gamma}{1+h/R} \, dt - F[V(t_2)] \tag{25}$$

The sum of R_I and R_F is the total range R_A. One of the results of this optimization technique is to find the velocities at the two ends of the constrained arc.

If it is found that $V(t_1) \leq V(t_2)$ then no path of finite length lies on the constraint boundary although the optimal path may coincide with the constraint boundary at a point. In this case there is no separation. However, for a given set of constraint levels an intermediate point constraint must be imposed [2], defined as $S(x, t_1) = 0$. The Lagrange multiplier associated with the intermediate constraint must be positive (for maximization); if it is not, an unconstrained path which lies below the constraint boundary will be better.

Necessary conditions for the two unconstrained arcs can be stated after first augmenting the performance indices as

$$\bar{R}_I = \Phi_I + \int_{t_o}^{t_1} [H - \lambda_v \dot{V} - \lambda_\gamma \dot{\gamma} - \lambda_h \dot{h}] \, dt \qquad (a)$$

$$\bar{R}_F = \Phi_F + \int_{t_2}^{t_f} [H - \lambda_v \dot{V} - \lambda_\gamma \dot{\gamma} - \lambda \dot{h}] \, dt \qquad (b) \qquad (26)$$

where

$$\Phi_I = F[V(t_1)] + \nu_h [h(t_1) - h_M] + \nu_\gamma \gamma(t_1) \qquad (a)$$

$$\Phi_F = -F[V(t_2)] + \bar{\nu}_h [h(t_f) - h_f] \qquad (b) \qquad (27)$$

and the variational Hamiltonian is

$$H = \frac{V \cos\gamma}{1+h/R} - \lambda_v \left[\frac{C_D \rho V^2 S}{2m} + g \sin\gamma \right] + \lambda_\gamma \left[\frac{C_L \rho V S}{2m} + \left(\frac{V}{R+h} - \frac{g}{V} \right) \cos\gamma \right] + \lambda_h V \sin\gamma \qquad (28)$$

Here $\lambda_v, \lambda_\gamma, \lambda_h, \nu_h, \nu_\gamma, \bar{\nu}_h$ are Lagrange multipliers. The Euler-Lagrange equations are defined from (28) as

$$\dot{\lambda}_v = -H_v, \quad \dot{\lambda}_\gamma = -H_\gamma, \quad \dot{\lambda}_h = -H_h \qquad (29)$$

The boundary conditions for the initial unconstrained problem at t_1 are

$$\lambda_v(t_1) = \Phi_{v(t_1)} = \left. \frac{2m}{\left(1 + \frac{h_M}{R}\right) C_D \rho_M V S} \right|_{t=t_1}, \quad \lambda_\gamma(t_1) = \Phi_{\gamma(t_1)} = \nu_\gamma, \quad \lambda_h(t_1) = \Phi_{h(t_1)} = \nu_h \qquad (30)$$

The boundary conditions for the terminal unconstrained problem at t_f are

$$\lambda_v(t_f) = \Phi_{v(t_f)} = 0, \lambda_\gamma(t_f) = \Phi_{\gamma(t_f)} = 0, \lambda_h(t_f) = \Phi_{h(t_f)} = \overline{\nu}_h \tag{31}$$

while at the exit corner

$$\lambda_{v(t_2)} = \Phi_{v(t_2)} = \left. \frac{2m}{(1 + \frac{h_M}{R})\ (C_D \rho_M VS)} \right|_{t = t_2} . \tag{32}$$

The original problem has been reduced to two, two-point boundary-value problems. For the initial arc the form of h, γ, and λ_v are known at the entry point and the initial conditions are given. For the terminal arc the form of h, γ, and λ_v, are known at the exit point whereas at the terminal boundary the values of λ_v, λ_γ, and h are known. Note that the problem is time-independent. This implies that $H = 0$ all along the optimum path.

In this example there are three state variables and a second order SVIC. Since the problem is time-independent $n-1 = p$.

6. CALCULATION OF THE PERFORMANCE INDEX ON THE CONSTRAINED ARC

An analytic expression cannot in general be found for the range when on the constraint boundary (23). However, when a successive improvement optimization scheme is used, some indication as to the improvement of the performance index is necessary. It is suggested that a table be made of range as a function of velocity starting at the largest expected value of $V(t_1)$

and ending at the lowest expected value of $V(t_2)$. The performance indices of (24) and (25) are written as $R_I - F(V_B)$ and $R_F + F(V_L)$ where V_B and V_L are chosen values in which on every iteration $V(t_1) > V_B$ and $V_L > V(t_2)$. Evaluating $F(V(t_1)) - F(V_B)$ and $F(V_L) - F(V(t_2))$ on the computer is reduced to a table look-up.

However, one important case where an analytic expression can be found for (23) is for the lift-drag polar defined as

$$C_L = C_{L_o} \alpha \tag{33}$$

$$C_D = C_{D_o} + C_{D_1} \alpha^2 \tag{34}$$

For values of the constants of $C_{L_o} = .020$, $C_{D_o} = .297$, $C_{D_1} = .451 \times 10^{-3}$ the lift-drag polar of Fig. 2 is obtained from (33) and (34). $\alpha(t)$ on the constraint boundary is now simply obtained from (33) and (22) as

$$\alpha = \frac{2m}{C_{L_o} \rho_M S} \left(\frac{g_M}{V^2} - \frac{1}{R + h_M} \right) \tag{35}$$

The drag coefficient of (34) is a function of velocity on the constraint

$$C_D = C_{D_o} + C_{D_1} \left[\frac{2m}{C_{L_o} \rho_M S} \right]^2 \left[\frac{g_M^2}{V^4} - \frac{2g_M}{(R + h_M)V^2} + \frac{1}{(R+h)^2} \right] \tag{36}$$

The analytic expression for the range on the constraint boundary solved by integrating (23) analytically is

$$R_A[t_1, t_2] = F[V(t_1)] - F[V(t_2)] =$$

$$\frac{RQ_1}{2} \left[\frac{1}{2Q_2} \log (Q_2 V^4 + Q_4 V^2 + Q_5) - \frac{Q_4}{Q_2 Q_6} \tan^{-1} \frac{2Q_2 V^2 + Q_4}{Q_6} \right] \tag{37}$$

where

$$Q_1 = \frac{2m}{(R + h_M)\,\rho_M S}\,,\quad Q_2 = C_{D_o} + \frac{C_{D_1}}{C_{L_o}^2}\,Q_1^2\,,\quad Q_3 = \frac{C_D g_M (R + h_M)}{C_{L_o}}$$

$$Q_4 = -\frac{2Q_3Q_1^2}{C_{L_o}}\,,\quad Q_5 = \frac{[Q_3Q_1]^2}{C_{D_1}}\,,\quad Q_o = \left(\frac{4C_{D_o}}{C_{D_1}}\right)^{\frac{1}{2}} Q_3Q_1$$

7. RE-ENTRY WITH G-LIMITING AND TOTAL HEATING CONSTRAINT

For practical reasons, the re-entry problem may be complicated further by additional constraints. One such constraint is a limit on the resultant aerodynamic force. The ratio of the resulting aerodynamic force to the sea level weight is defined here as the number of g's,

$$N_g \equiv \frac{\sqrt{L^2 + D^2}}{mg_o} \tag{38}$$

If N_g is required to be less than some given number, this imposes a control variable inequality constraint on the trajectory. This constraint can be handled by the techniques of reference 2. It presents no obstacle to the separation of arcs as long as g-limit is always satisfied along the constraint boundary.

Another practical constraint is a limit on the total heat absorbed by the heat shield. If the total heating is constrained the arcs cannot be separated in the maximum range problem with an altitude constraint. The amount of heat absorbed on one arc determines the amount of heat that can be absorbed on the other arc. The arcs are now dependent upon each other and the more complicated technique of reference 5 can be used. However, an alternative

approach is to perform a parameter search on an equivalent problem that does separate. The heating rate is

$$\dot{q} = C_q \rho^{\frac{1}{2}} V^3 \tag{39}$$

where q is the heat and C_q is a known constant. A composite performance index can be formed using (39) and (18) as

$$R_q = \int_{t_o}^{t_f} \left[\frac{V \cos \gamma}{1 + h/R} - KC_q \rho^{\frac{1}{2}} V^3 \right] dt \tag{40}$$

The procedure for finding optimal paths with a heating constraint is as follows: Choose a value for K. Since the problem is separable, the optimal arcs can easily be found and the total heat evaluated. If the value of total heating is greater than the desired value, K is increased; if less than the desired value, K is decreased. For a new value of K the optimal arcs and the total heating are again evaluated. This search for the proper value of K is continued until the desired value of total heating is attained.

In general, integral constraints (the heating constraint above is an example) may be handled by this procedure.

8. NUMERICAL DETERMINATION OF MAXIMUM RANGE TRAJECTORIES

Numerical Methods The "Conjugate Gradient Method" of reference 4, was used to determine the two unconstrained arcs of the re-entry problem.

To check the results of the Conjugate Gradient Method a second order optimization program, the "successive sweep method" of references 6 and 8, was used. This latter algorithm generates a sequence of improving paths

by maximizing a quadratic approximation to the performance index.

Intitial Arc The initial conditions for this arc were taken as: V = 33,961 ft./sec., γ = - 1.57 deg., and h = 189,890 ft. The terminal conditions at the entry point ($t = t_1$) onto the constraint boundary are h = 220,000 ft. and $\gamma = 0$ (V and t_1 are unspecified). The equations of motion were integrated forward from the given initial conditions until γ becomes zero for the second time. In the conjugate gradient method the altitude constraint at the end of the arc was met using a quadratic penalty function. At that point λ_γ was determined by setting the Hamiltonian equal to zero. Convergence was achieved in seven iterations using less than 15 seconds per iteration on the IBM 7094 computer. Fig. 4 shows, in altitude-range space, the starting nominal and some of the following iterations.

However, the trajectory of Fig. 4 is not the optimum path; it is only a local optimum. Fig. 5 shows this path with another locally optimum path that gives 30% more range for the initial arc down to a velocity of 26,494 ft./sec (from this velocity on, the maximum range paths are the same). The increase in range over the entire flight is 6%. The existence of two locally optimal paths was not detected in either reference 11 or 5.

These two paths arise from widely different control strategies (See Fig. 7). Path 2 in Fig. 5, 6, and 7 uses low angles-of-attack to keep the drag small and consequently penetrates deeply into the atmosphere where air density is high. Path 1 uses larger values of angle-of-attack to keep the vehicle at higher altitudes where air density and drag are lower. Path 1 seems to concentrate on maximizing $F[V(t_1)]$ in Eqn. (24) whereas path 2 seems to

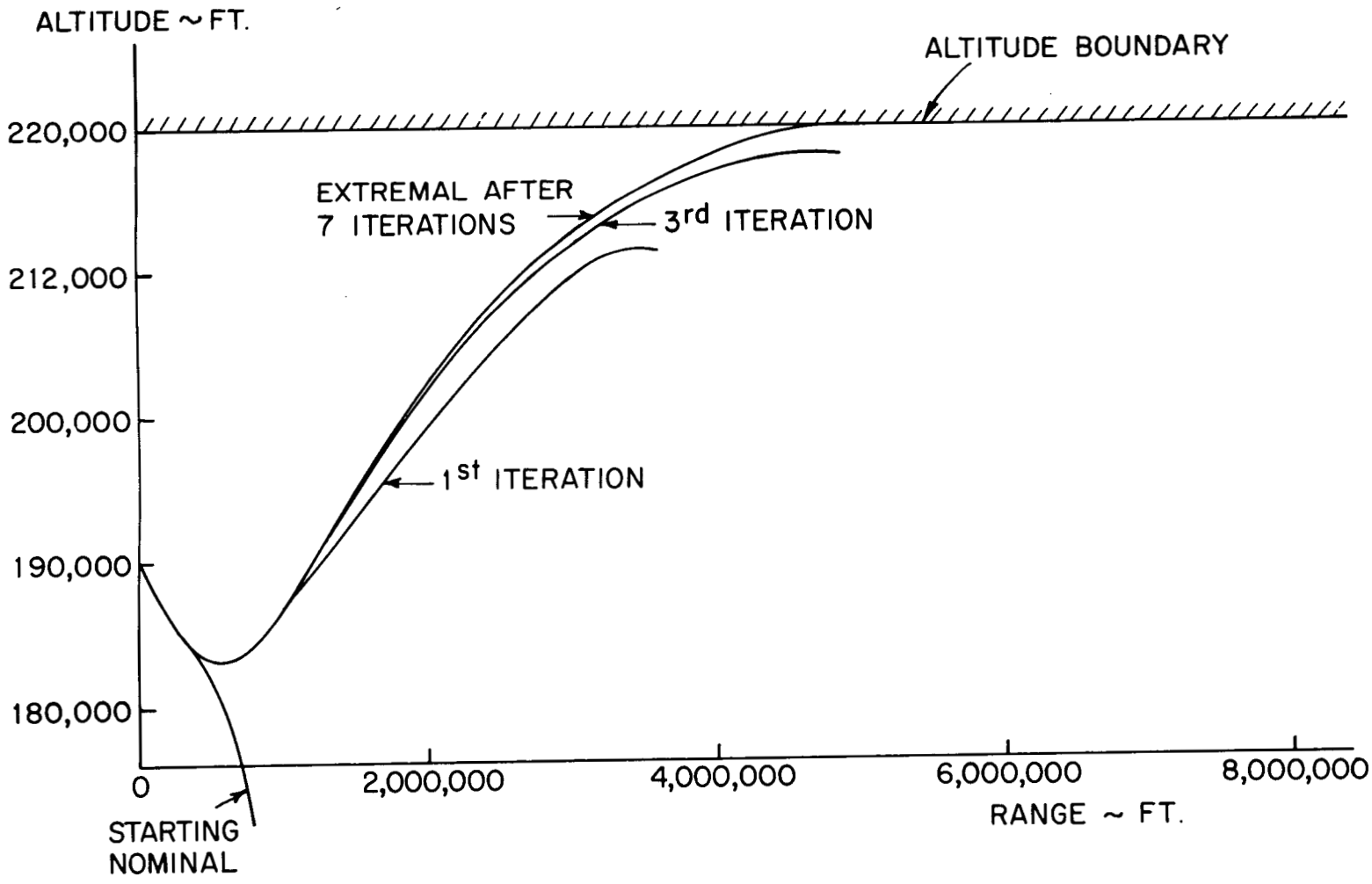

FIG. 4 LOCALLY OPTIMUM MAXIMUM RANGE TRAJECTORY FOR INITIAL PHASE OF RE-ENTRY. SEVEN ITERATIONS OF CONJUGATE GRADIENT METHOD USED TO CONVERGE TO THE EXTREMAL PATH.

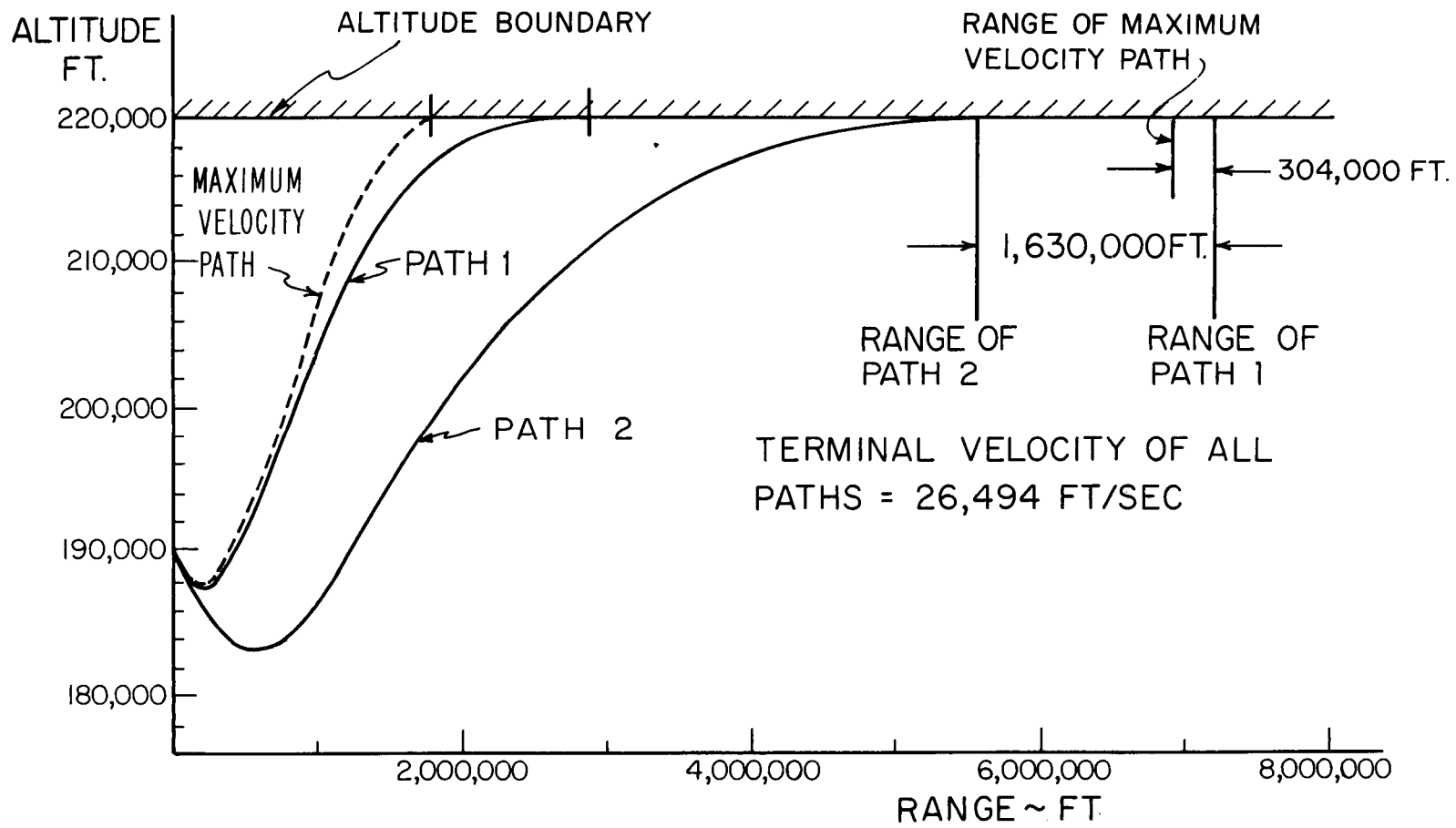

FIG. 5 TWO LOCALLY MAXIMUM RANGE TRAJECTORIES FOR THE INITIAL PHASE OF RE-ENTRY IN ALTITUDE-RANGE SPACE.

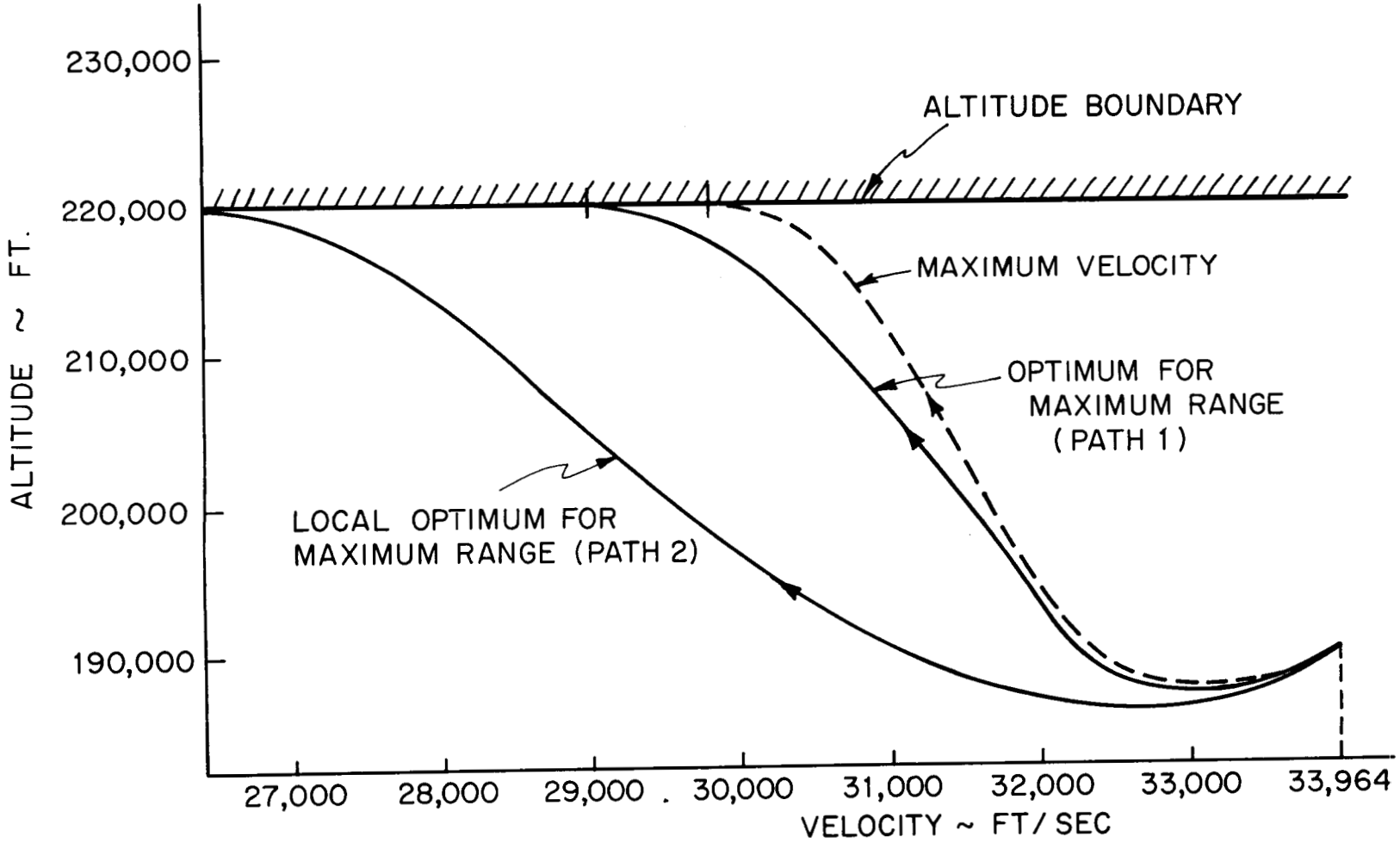

FIG. 6 TWO LOCALLY MAXIMUM RANGE TRAJECTORIES FOR THE INITIAL PHASE OF RE-ENTRY IN ALTITUDE-VELOCITY SPACE.

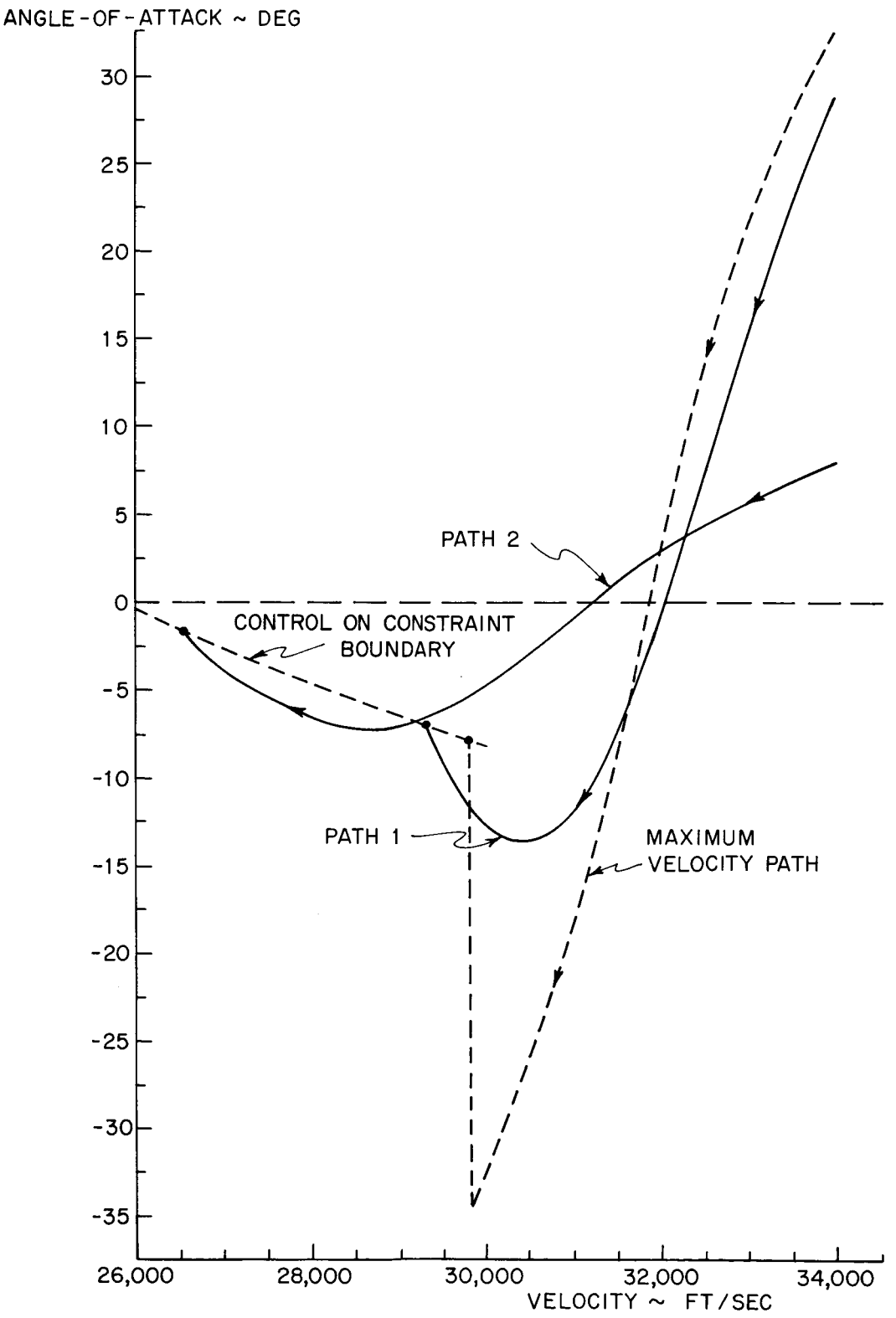

FIG. 7 ANGLE-OF-ATTACK Vs. VELOCITY FOR TWO LOCALLY MAXIMUM RANGE PATHS.

concentrate on maximizing the integral (the range) in Eqn (24). Path 1 and 2 are shown in Fig. 6 in altitude-velocity space.

Continuity of the α- Program Results obtained in reference 5 show a discontinuity in the α-program at the entry point onto the constrained arc. The control should be continuous since the variational Hamiltonian is regular [11]. The performance index is not very sensitive to this discontinuity so first order methods have great difficulty in obtaining continuous α-programs. The second order scheme demonstrates clearly that α is continuous across the entry point for path 1.

Maximum Velocity Path The trade off between entry point velocity and range in the performance index suggests that the maximum velocity path may be a good approximation to the maximum range path. The maximum velocity path is shown by a dashed path in Figs. 5, 6, and 7. The maximum velocity path (Fig. 5) plus the constrained path down to 26,494 ft/sec. gives only 5.5% less range than path 1 and 24.5% more range than path 2. Initially, the angle-of-attack program for maximum velocity resembles that of path 1, (Fig. 7), however, as the paths near the entry point, α for path 1 bends over. The difference in velocity at the entry point between the maximum velocity path and path 1 is 520 ft/sec. as seen in Fig. 6.

Conjugate Point First-order computing methods try to improve performance index on each iteration, without concern for the change in the size of the gradient. They will not converge to an extremal path that contains a conjugate point, since such a path is not an optimal path.

An attempt was made, using the second-order sweep method to check the results obtained for path 2 of Fig. 5 by the first-order conjugate gradient method. However, all attempts at solution of the matrix Riccati equation (which governs the second partial derivatives of the optimal return function with respect to the state variables) resulted in overflow of the computer (10^{38}). This led us to suspect the presence of conjugate points in the vicinity of the extremal field for the following reasons:

(a) Using the conjugate gradient method to solve the maximum range problem, both the performance index and the norm of the gradient increased for some iterations. This behavior indicates that a conjugate point might exist.

(b) The sweep method tries to decrease the magnitude of the gradient on each iteration, without concern for the change in the performance index. Hence, the method may very well move toward an extremal path containing a conjugate point; however, convergence to such a path will <u>not</u> be obtained, because solutions to the Ricatti equation, as mentioned above, will overflow the computer first.

(c) A necessary (but <u>not</u> sufficient) condition for the existence of a conjugate point on an extremal path in a maximization problem is for the matrix

$$B \triangleq H_{xx} - H_{x\alpha} H_{\alpha\alpha}^{-1} H_{\alpha x} \tag{41}$$

to have some positive eigenvalues over all or part of the path (cf. refs. 7 and 9). If B is negative-definite over the whole path there can be no conjugate points. For both paths 1 and 2 in Fig. 5 we found that B did indeed have some positive eigenvalues.

Terminal Arc At neither end of the terminal arc are all the state variables specified. In the conjugate gradient method the missing initial conditions are treated as control parameters chosen to maximize the objective function. At the initial point of the terminal arc h and γ are known but V is to be determined. From (25) and (32)

$$\left.\frac{\partial R_F}{\partial V}\right|_{t = t_2} = \lambda_v(t_2) - \frac{1}{(1 + \frac{h_M}{R})(\frac{C_D \rho_M V S}{2m})} \tag{42}$$

The optimization process drives $\frac{\partial R_F}{\partial V}$ to zero making $\lambda_v(t_2)$ equal to the required value.

The optimal path obtained is shown in Fig. 8 in the altitude-range space. The α-program corresponds very closely to the α for maximum L/D (lift over-drag ratio) except near the terminal point where high values of angle-of-attack are used in the flare-out maneuver. Fig. 9 shows the α history as a function of range. The exit velocity determined by a parameter search is 19,010 ft/sec.

9. CONCLUSIONS

A sufficient condition for separate computation of arcs for certain optimization problems with state variable inequality constraints was formally presented. This concept was applied to the problem of maximizing the range of a glider entering the Earth's atmosphere at parabolic speeds subject to a maximum altitude constraint after the initial pull up. In numerically determining the unconstrained arcs, the conjugate gradient method converged extremely rapidly. This allowed a detailed investigation of maximum range

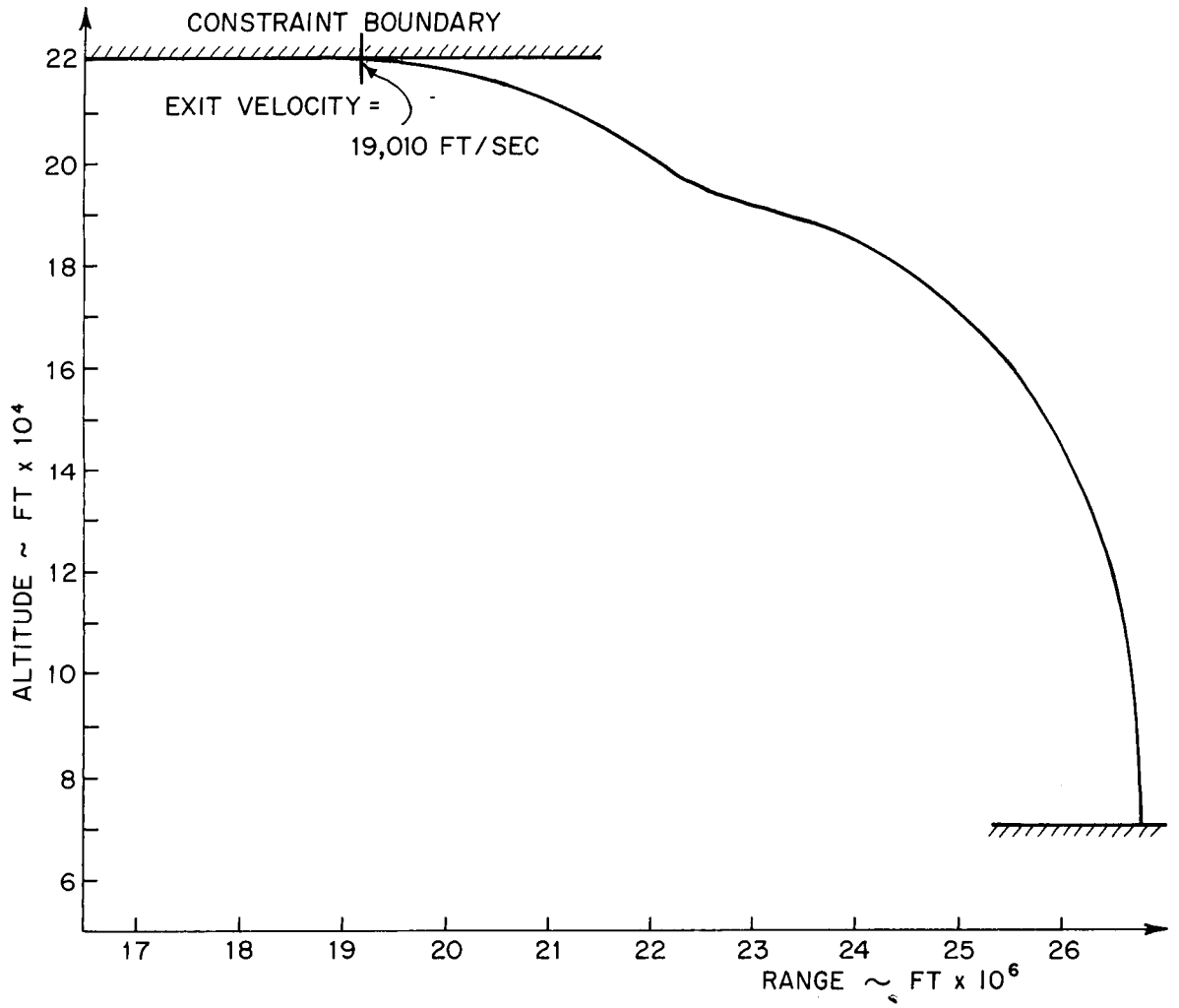

FIG. 8 ALTITUDE vs. RANGE FOR THE TERMINAL PHASE OF RE-ENTRY PROBLEM.

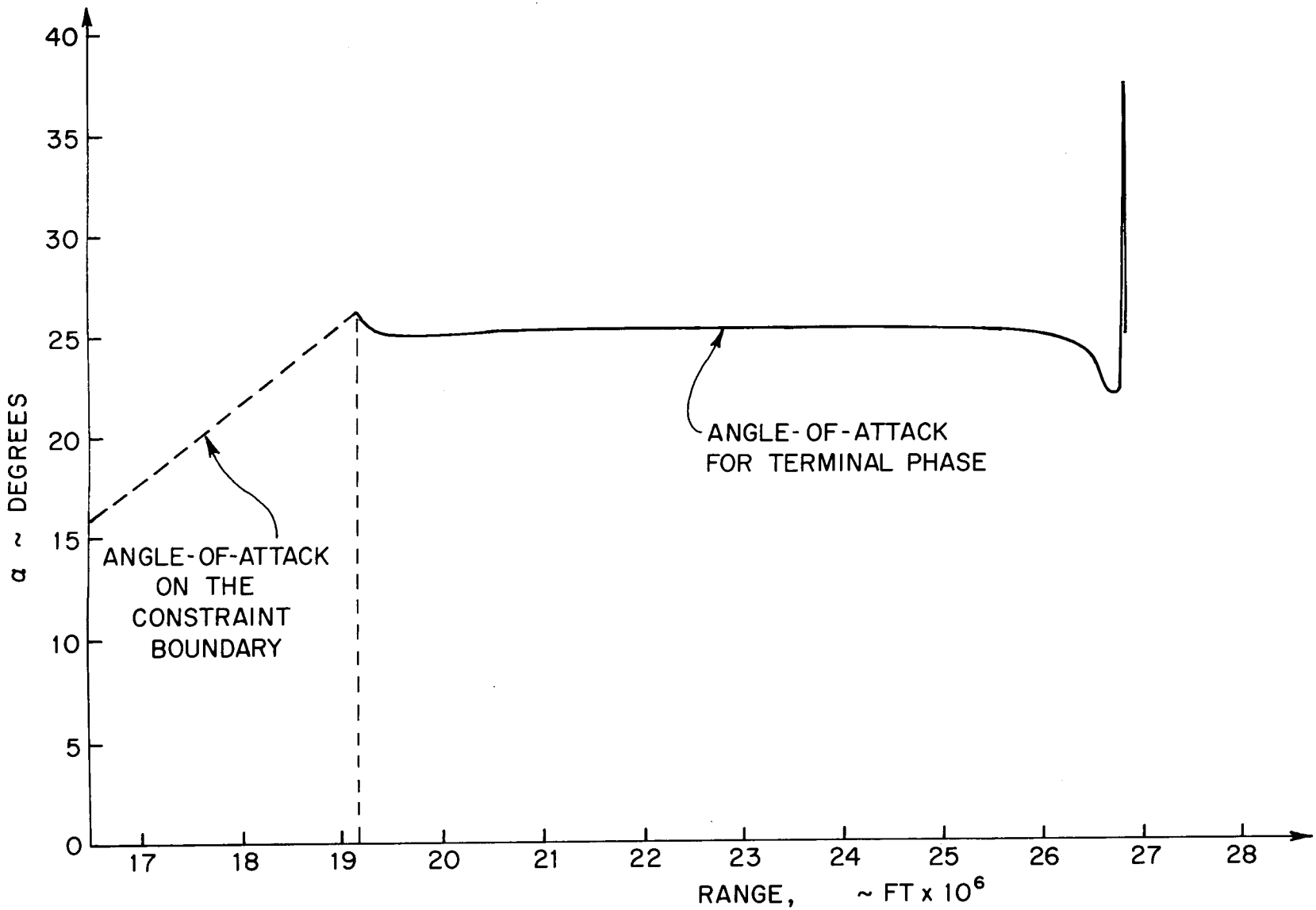

FIG. 9 ANGLE-OF-ATTACK PROGRAM FOR THE TERMINAL PHASE OF THE RE-ENTRY PROBLEM.

Academy Library (DFSLB)
U. S. Air Force Academy
Colorado Springs, Colorado 80912

AEDC (AEO, INC)
Attn: Library/Documents
Arnold AFS, Tenn 37389

Aeronautics Library
Graduate Aeronautical Laboratories
California Institute of Technology
1201 E. California Blvd.
Pasadena, California 91109

Aerospace Corporation
P. O. Box 95085
Los Angeles, Calif 90045
Attn: Library Acquisitions Group

Airborne Instruments Laboratory
Deerpark, New York 11729

AFAL (AVTE/ R.D. Larson)
Wright-Patterson AFB
Ohio 45433

AFCRL (CRMCLR)
AFCRL Research Library, Stop 29
L. G. Hanscom Field
Bedford, Mass. 01731

AFETR (ETLLG-1)
STINFO Officer (for library)
Patrick AFB, Florida 32925

AFETR Technical Library
(ETV, MU-135)
Patrick AFB, Florida 32925

AFFTC (FTBPP-2)
Technical Library
Edwards AFB, California 93523

AFGC (FWBRS-12)
Eglin AFB
Florida 32542

AFL (ARIY)
Wright-Patterson AFB
Ohio 45433

AUL3T-9663
Maxwell AFB
Alabama 36112

Mr. Henry L. Bachmann
Assistant Chief Engineer
Wheeler Laboratories
122 Cuttermill Road
Great Neck, New York 11021

Bendix Pacific Division
11600 Sherman Way
North Hollywood, California 91605

Colonel A. D. Blue
RTD (RTTL)
Bolling Air Force Base, D. C. 20332

California Institute of Technology
Pasadena, California 91109
Attn: Documents Library

Carnegie Institute of Technology
Electrical Engineering Dept.
Pittsburgh, Pa 15213

Central Intelligence Agency
Attn: OCR/DD Publications
Washington, D. C. 20505

Chief of Naval Operations
OP-07
Washington, D. C. 20350

Chief of Naval Research
Department of the Navy
Washington, D. C. 20360
Attn: Code 427

Commandant
U. S. Army and General Staff College
Attn: Secretary
Fort Leavenworth, Kansas 66270

Commander
Naval Air Development and
Material Center
Johnsville, Pennsylvania 18974

Commanding General
Frankford Arsenal
Attn: SMUFA-L6000 (Dr. Sidney Ross)
Philadelphia, Pa. 19137

Commandant
U. S. Army Air Defense School
Attn: Missile Sciences Div. C & S Dept.
P. O. Box 9390
Fort Bliss, Texas 79916

Commander
U. S. Naval Air Missile Test Center
Point Mugu, California 93041

Commanding General
Attn: STEWS-S-VT
White Sands Missile Range
New Mexico 88002

Commanding General
U. S. Army Electronics Command
Fort Monmouth, New Jersey 07703

Attn: AMSEL-SC
RD-D
RD-G
RD-GF
RD-MAT
XL-D
XL-E
XL-C
XL-S
HL-D
HL-CT-E
HL-CT-P
HL-CT-L
HL-CT-O
HL-CT-I
HL-CT-A
ML-D
ML-A
ML-P
ML-R
NL-S
KL-D
KL-E
KL-S
KL-T
VL-D
WL-D

Commanding General
U. S. Army Material Command
Attn: AMCRD-RS-DE-E
Washington, D. C. 20315

Commanding General
U. S. Army Missile Command
Attn: Technical Library
Redstone Arsenal, Alabama 35809

Commanding Officer
Naval Avionics Facility
Indianapolis, Indiana 46241

Commanding Officer
Naval Ordnance Laboratory
Corona, California 91720

Commanding Officer
Naval Ordnance Laboratory
White Oak, Maryland 21502

Commanding Officer
Naval Ordnance Test Station
China Lake, California 93555

Commanding Officer
Naval Training Device Center
Orlando, Florida 32811

Commanding Officer
Office of Naval Research Branch Office
1030 East Green Street
Pasadena, California

Commanding Officer
Office of Naval Research Branch Office
219 South Dearborn Street
Chicago, Illinois 60604

Commanding Officer
Office of Naval Research Branch Office
495 Summer Street
Boston, Massachusetts 02210

Commanding Officer
Office of Naval Research Branch Office
207 West 24th Street
New York, New York 10011

Commanding Officer
Office of Naval Research Branch Office
Box 39, Navy No. 100 F. P. O.
New York, New York 09510

Commanding Officer
U. S. Army Electronics R & D Activity
Fort Huachuca, Arizona 85613

Commanding Officer
U. S. Army Electronics R & D Activity
White Sands Missile Range
New Mexico 88002

Commanding Officer
U. S. Army Engineer R & D Laboratory
Attn: STINFO Branch
Fort Belvoir, Virginia 22060

Commanding Officer
U. S. Army Research Office (Durham)
Attn: CRD-AA-IP (Richard O. Ulsh)
Box CM, Duke Station
Durham, North Carolina 27706

Commanding General
U. S. Army Strategic Communications
Command
Washington, D. C. 20315

Commanding Officer
Harry Diamond
Attn: Dr. Berthold Altman (AMXDO-TI)
Connecticut Avenue & Van Ness Street NW
Washington, D. C. 20438

Commanding Officer
Human Engineering Laboratories
Aberdeen Proving Ground, Maryland 21005

Commanding Officer
U. S. Army Ballistics Research Laborat.
Attn: V. W. Richards
Aberdeen Proving Ground
Aberdeen, Maryland 21005

Commanding Officer
U. S. Army Limited War Laboratory
Attn: Technical Director
Aberdeen Proving Ground
Aberdeen, Maryland 21005

Commanding Officer
U. S. Army Materials Research Agency
Watertown Arsenal
Watertown, Massachusetts 02172

Commanding Officer
U. S. Army Security Agency
Arlington Hall
Arlington, Virginia 22212

Commanding Officer and Director
U. S. Naval Underwater Sound Lab.
Fort Trumbull
New London, Connecticut 06840

Defense Documentation Center
Attn: TISIA
Cameron Station, Bldg. 5
Alexandria, Virginia 22314

Det #6, OAR (LODAR)
Air Force Unit Post Office
Los Angeles, Calif. 90045

Director
Advanced Research Projects Agency
Department of Defense
Washington, D. C. 20301

Director for Materials Sciences
Advanced Research Projects Agency
Department of Defense
Washington, D. C. 20301

Director
Columbia Radiation Laboratory
Columbia University
538 West 120th Street
New York, New York 10027

Director
Coordinated Science Laboratory
University of Illinois
Urbana, Illinois 61803

Director
Electronics Research Laboratory
University of California
Berkeley, California 94720

Director
Electronic Sciences Laboratory
University of Southern California
Los Angeles, California 90007

Director
Microwave Laboratory
Stanford University
Stanford, California 94305

Director - Inst. for Exploratory
Research
U. S. Army Electronics Command
Attn: Dr. Robert O. Parker, Executive
Secretary, JSTAC (AMSEL-XL-D)
Fort Monmouth, New Jersey 07703

Director
National Security Agency
Attn: Librarian C-332
Fort George G. Meade, Maryland 20755

Director, Naval Research Laboratory
Technical Information Officer
Washington, D. C.
Attn: Code 2000

Director
Research Laboratory of Electronics
Massachusetts Institute of Technology
Cambridge, Mass. 02139

Director
Stanford Electronics Laboratories
Stanford University
Stanford, California 94305

Director, USAF Project RAND
Via: Air Force Liaison Office
The RAND Corporation
1700 Main St., Santa Monica, Cal. 90406
Attn: Library

Director
U. S. Army Engineer Geodesy,
Intelligence and Mapping
Research and Development Agency
Fort Belvoir, Virginia 22060

Director
U. S. Naval Observatory
Washington, D. C. 20390

Director, U. S. Naval Security Group
Attn: G43
3801 Nebraska Avenue
Washington, D. C. 20390

Division of Engineering and Applied
Physics
210 Pierce Hall
Harvard University
Cambridge, Massachusetts 02138

Professor A. A. Dougal, Director
Laboratories for Electronics and
Related Sciences Research
University of Texas
Austin, Texas 78712

ESD (ESTI)
L. G. Hanscom Field
Bedford, Mass. 01731

European Office of Aerospace Research
Shell Building
47 Rue Cantersteen
Brussels, Belgium

Colonel Robert L. Fontana
Department of Electrical Engineering
Air Force Institute of Technology
Wright-Patterson AFB, Ohio 45433

General Electric Co.
Research Laboratories
Schenectady, New York 12301

Professor Nicholas George
California Inst. of Technology
Pasadena, California 91109

Goddard Space Flight Center
National Aeronautics and Space Admin.
Attn: Library, Documents Section
Code 252
Green Belt, Maryland 20771

Dr. John C. Hancock, Director
Electronic Systems Research Laboratory
Purdue University
Lafayette, Indiana 47907

Dr. D. Harrison, Code RRE
Chief, Electrophysics Branch
National Aeronautics and Space
Administration
Washington, D. C. 20546

Head, Technical Division
U. S. Naval Counter Intelligence
Support Center
Fairmont Building
4420 North Fairfax Drive
Arlington, Virginia 22203

Headquarters
Defense Communications Agency
The Pentagon
Washington, D. C. 20305

Dr. L. A. Hollingsworth
AFCRL (CRI)
L. G. Hanscom Field
Bedford, Massachusetts 01731

Hunt Library
Carnegie Institute of Technology
Schenley Park
Pittsburgh, Pa. 15213

The Johns Hopkins University
Applied Physics Laboratory
8621 Georgia Avenue, Silver Spring, Md.
Attn: Boris W. Kuvshinoff 20910
Document Librarian

Lt. Col Robert B. Kalisch
Chief, Electronics Division
Directorate of Engineering Sciences
Air Force Office of Scientific Research
Arlington, Virginia 22209

Colonel Kee
AFRSTE
Hqs. USAF
Room ID-429, The Pentagon
Washington, D. C. 20330

Dr. S. Benedict Levin, Director
Institute for Exploratory Research
U. S. Army Electronics Command
Fort Monmouth, New Jersey 07703

Los Alamos Scientific Laboratory
Attn: Reports Library
P. O. Box 1663
Los Alamos, New Mexico 87544

Librarian
U. S. Naval Electronics Laboratory
San Diego, California 95152

Librarian
U. S. Navy Post Graduate School
Monterey, California 93940

Lockheed Aircraft Corp
P. O. Box 504
Sunnyvale, California 94088

Dr. I. R. Mirman
AFSC (SCT)
Andrews Air Force Base, Maryland 20331

Lt. Col Bernard S. Morgan
Frank J. Seiler Research Laboratory
U. S. Air Force Academy
Colorado Springs, Colorado 80912

Dr. G. J. Murphy
The Technological Institute
Northwestern University
Evanston, Illinois 60201

Mr. Peter Murray
Air Force Avionics Laboratory
Wright-Patterson AFB, Ohio 45433

NASA Lewis Research Center
Attn: Library
21000 Brookpark Road
Cleveland, Ohio 44135

NASA Scientific & Technical
Information Facility
Attn: Acquisitions Branch (S/AK/DL)
P. O. Box 33
College Park, Maryland 20740

National Science Foundation
Attn: Dr. John R. Lehmann
Division of Engineering
1800 G Street, N. W.
Washington, D. C. 20550

National Security Agency
Attn: R4-James Tippet
Office of Research
Fort George G. Meade, Maryland 20755

Naval Air Systems Command
AIR 03
Washington, D. C. 20360

Naval Electronics Systems Command
ELEX 03
Falls Church, Virginia 22046

Naval Ordnance Systems Command
ORD 32
Washington, D. C. 20360

Naval Ordnance Systems Command
SHIP 035
Washington, D. C. 20360

Naval Ship Systems Command
SHIP 031
Washington, D. C. 20360

New York University
College of Engineering
New York, New York 10019

Dr. H. V. Noble
Air Force Avionics Laboratory
Wright-Patterson AFB, Ohio 45433

Office of Deputy Director
(Research and Information Rm. 3D1037)
Department of Defense
The Pentagon
Washington, D. C. 20301

Polytechnic Institute of Brooklyn
55 Johnson Street
Brooklyn, New York 11201
Attn: Mr. Jerome Fox
Research Coordination

RADC (EMLAL-1)
Griffiss AFB, New York 13442
Attn: Documents Library

Raytheon Co
Bedford, Mass. 01730
Attn: Librarian

Lt. Col. J. L. Reeves
AFSC (SCSB)
Andrews Air Force Base, Md 20331

Dr. Edward W. Reilley
Asst. Director (Research)
Offc. of Defense Res. & Eng.
Department of Defense
Washington, D. C. 20301

Research Plans Office
U. S. Army Research Office
3045 Columbia Pike
Arlington, Virginia 22204

Dr. H. Robl, Deputy Chief Scientist
U. S. Army Research Office (Durham)
Durham, North Carolina 27706

Emil Schafer, Head
Electronics Properties Info Center
Hughes Aircraft Co
Culver City, California 90230

School of Engineering Sciences
Arizona State University
Tempe, Arizona 85281

Space Systems Division
Air Force Systems Command
Los Angeles Air Force Station
Los Angeles, California 90045
Attn: SSSD

SSD (SSTRT/Lt. Starbuck)
AFUPO
Los Angeles, California 90045

Superintendent
U. S. Army Military Academy
West Point, New York 10996

Colonel A. Swan
Aerospace Medical Division
Brooks Air Force Base, Texas 78235

Syracuse University
Department of Electrical Engineering
Syracuse, New York 13210

Systems Engineering Group (RTD)
Technical Information Reference Branch
Attn: SEPIR
Direct. of Sys. Stand & Tech. Inf.
Wright-Patterson AFB, Ohio 45433

University of California
Santa Barbara, California 93106
Attn: Library

University of California at Los Angeles
Department of Engineering
Los Angeles, California 90024

University of Michigan
Electrical Engineering Dept.
Ann Arbor, Michigan 48104

U. S. Army Munitions Command
Attn: Technical Information Branch
Picatinney Arsenal
Dover, New Jersey 07801

U. S. Army Research Office
Attn: Physical Sciences Division
3045 Columbia Pike
Arlington, Virginia 22204

U. S. Atomic Energy Commission
Division of Technical Information Ext.
P. O. Box 62
Oak Ridge, Tenn. 37831

U. S. Naval Weapons Laboratory
Dahlgren
Virginia 22448

Major Charles Waespy
Technical Division
Deputy for Technology
Space Systems Division, AFSC
Los Angeles, California 90045

The Walter Reed Institute of Research
Walter Reed Medical Center
Washington, D. C. 20012

Colonel J. B. Warthman
AFSC (SCTR)
Andrews Air Force Base, Maryland 20331

Weapons Systems Test Division
Naval Air Test Center
Patuxent River, Maryland 20670
Attn: Library

Weapons Systems Evaluation Group
Attn: Col. Daniel W. McElwee
Department of Defense
Washington, D. C. 20305

Yale University
Engineering Department
New Haven, Connecticut 06720

Mr. Charles F. Yost
Special Assistant to the Director of
Research
National Aeronautics and Space Admin.
Washington, D. C. 20546

Dr. Leo Young
Stanford Research Institute
Menlo Park, California 94025

trajectories.

For the initial phase of re-entry two locally maximum range arcs were found. This appears to be a consequence of the lift-drag characteristics of the vehicle and the decrease in air density with altitude. Both first and second order methods indicate a conjugate point behavior in the initial phase extremal field.

REFERENCES

1. Gamkrelidze, R. V. "Optimal Processes with Bounded Phase Coordinates," Izv. Akad. Nauk. USSR, Sec. Mat., Vol. 24, pp. 315-356, 1960.

2. Bryson, A. E. Jr., Denham, W. F., Dreyfus, S. E., "Optimal Programming Problems with Inequality Constraints I: Necessary Conditions for Extremal Solutions," AIAA Journal, Vol. 1, No. 11, November, 1963.

3. Kelley, H. J. "Method of Gradients," Ch. 6 of Optimization Techniques, edited by G. Leitmann, Academic Press, New York, N.Y., 1962.

4. Lasdon, L. S., Mitter, S. K., Warren, A. D., "The Method of Conjugate Gradient for Optimal Control Problems," Proc. IEEE, p. 904, June 1966.

5. Denham, W. F., Bryson, A. E. Jr., "Optimal Programming Problems with Inequaltiy Constraints II: Solution by Steepest-Ascent" AIAA Journal Vol. 2, No. 1, January 1964.

6. McReynolds, S. and Bryson, A. E. Jr., "A Successive Sweep Method for Solving Optimal Programming Problems," Sixth Joint Automatic Control Conference, Troy, New York, June 1965.

7. Breakwell, J. V. and Ho, Y. C., "On the Conjugate Point Condition for the Control Problem," Int. Journal of Engineering, Vol. 2, pp. 565-579, 1965.

8. Mitter, S. K., "Successive Approximation Methods for the Solution of Optimal Control Problems," Automatica, Vol. 3, pp. 135-149, 1966.

9. Bryson, A. E. Jr., and Ho, Y. C., "Optimization, Estimation, and Control," Lecture Notes, Harvard University, 1966-1967.

10. Paiewonsky, Bernard, "On Optimal Control with Bounded State Variables," Aeronautical Research Associates of Princeton, Inc. Report No. 60. July 1964.

11. Lasdon, Warren, and Rice, "An Interior Penalty Function Method for Inequality Constrained Optimal Control Problem," Case Institute of Technology, Cleveland, Ohio, November 1966.

Unclassified
Security Classification

DOCUMENT CONTROL DATA - R & D

Security classification of title, body of abstract and indexing annotation must be entered when the overall report is classified)

1. ORIGINATING ACTIVITY (Corporate author)

Division of Engineering and Applied Physics
Harvard University Cambridge, Massachusetts

2a. REPORT SECURITY CLASSIFICATION

Unclassified

2b. GROUP

3. REPORT TITLE

THE SEPARATE COMPUTATION OF ARCS FOR OPTIMAL FLIGHT PATHS WITH STATE VARIABLE INEQUALITY CONSTRAINTS

4. DESCRIPTIVE NOTES (Type of report and inclusive dates)

Interim technical report

5. AUTHOR(S) (First name, middle initial, last name)

Jason L. Speyer, Raman K. Mehra, and Arthur E. Bryson, Jr.

6. REPORT DATE	7a. TOTAL NO. OF PAGES	7b. NO. OF REFS
May 1967	31	11

8a. CONTRACT OR GRANT NO.	9a. ORIGINATOR'S REPORT NUMBER(S)
Nonr-1866(16) & NASA Grant NGR-22-007-068	Technical Report No. 526
b. PROJECT NO.	
c.	9b. OTHER REPORT NO(S) (Any other numbers that may be assigned this report)
d.	

10. DISTRIBUTION STATEMENT

Reproduction in whole or in part is permitted by the U. S. Government. Distribution of this document is unlimited.

11. SUPPLEMENTARY NOTES	12. SPONSORING MILITARY ACTIVITY
	Office of Naval Research

13. ABSTRACT

Separate computation of arcs is possible for a large class of optimization problems with state variable inequality constraints. Surprisingly, this class (to the best of the authors' knowledge) includes all physical problems which have been solved analytically or numerically to date. Typically thse problems have only one constrained arc. Even in more complex problems, separation of arcs can be used to search for additional constrained arcs.

As an important example,a maximum range trajectory for a glider entering the Earth's atmosphere at a supercircular velocity is determined, subject to a maximum altitude constraint after initial pull-up. It is shown that the optimal path can be divided into three arcs, which may be determined separately with no approximations. The three arcs are (1) the initial arc, beginning at specified initial condition and ending at the entry point onto the altitude constraint; (2) the arc lying on the altitude constraint; and (3) the terminal arc, beginning at the exit point of the altitude constraint and ending at some specified terminal altitude.

The conjugate gradient method, (ref. 4), a first order optimization scheme is shown to converge very rapidly to the individual unconstrained optimal arcs. Using this optimization scheme and taking advantage of the separation of arcs an investigation revealed that two locally optimum paths exist. The range of one exceeds the range of the other by about 250 nautical miles (about 6%) for the re-entry vehicle used here (maximum lift-to-drag ratio is .9) .

14 KEY WORDS	LINK A		LINK B		LINK C	
	ROLE	WT	ROLE	WT	ROLE	WT
separate computation of arcs optimal flight paths state variable inequality constraints						